State-Specific Reactions of $Fe^+(a^6D,a^4F)$ with D_2O and Reactions of FeO^+ with D_2

D. E. Clemmer,† Yu-Min Chen, Farooq A. Khan, and P. B. Armentrout*

Department of Chemistry, University of Utah, Salt Lake City, Utah 84112

Received: February 3, 1994; In Final Form: April 26, 1994®

Reactions of Fe^+ with D_2O and FeO^+ with D_2 are studied as a function of translational energy in a guided-ion beam tandem mass spectrometer. In the former system, the only products observed from single-collision events are FeD^+ and $FeOD^+$. These products are formed in endothermic reactions. At low energies, the $FeOD_2^+$ adduct is also observed, a result of secondary stabilizing collisions with D_2O. Results for Fe^+ produced in two different sources are analyzed to yield state-specific cross sections for reaction of the a^6D ground and a^4F first excited states of Fe^+. In the reaction of FeO^+ with D_2, three ionic products (Fe^+, FeD^+, and $FeOD^+$) are observed. An inefficient exothermic process that forms $Fe^+ + D_2O$ is observed, consistent with known thermochemistry; however, formation of $Fe^+ + D_2O$ also occurs via another more efficient pathway that involves a reaction barrier of ~0.6 eV. The $FeOD^+$ channel also proceeds via a pathway involving a reaction barrier of the same energy. Results for both the $Fe^+ + D_2O$ and $FeO^+ + D_2$ systems are used to derive potential energy surfaces for these systems.

Introduction

Transition metal–oxide and –hydroxide species are of interest in basic research and areas involving catalysis.[1] For example, in the condensed phase, iron(IV and V) oxide catalysts and other metal oxide catalysts have been used to convert alkanes to alcohols, a process that is of economic interest. One mechanism that has been proposed to explain this behavior involves formation of metal–hydroxide (R–M–OH) intermediates.[1-4] Comparable intermediates have also been proposed for the reaction of FeO^+ with hydrocarbons in the gas phase;[5-8] however, little is known about the detailed steps associated with the mechanism for these reactions. Furthermore, the thermochemistry of these proposed hydroxide intermediates and the critical transition states along the reaction pathway remain largely unstudied.

In this work, we report on the energetics associated with formation of ionic $FeOD^+$ from the reaction Fe^+ with D_2O and FeO^+ with D_2. These reactions, which involve only four atoms, are the simplest possible bimolecular processes that can lead to metal–hydroxide formation. Therefore, they offer an opportunity to discern the detailed reaction mechanisms and to probe the potential energy surfaces of this system, in particular, to specify the location and magnitude of any rate-limiting reaction barriers. Here, we derive cross sections for state-specific reactions of water with the $Fe^+(a^6D)$ ground and $Fe^+(a^4F)$ first excited states. State-specific data involving Fe^+ have been obtained previously for reactions with hydrogen[9] and small alkanes.[10-12] These data have led to a detailed understanding of the electronic constraints associated with these reactions.

Another purpose of these studies is to gain a better understanding of the dehydrogenation process in the $Fe^+ + D_2O$ reaction. Dehydrogenation of small hydrocarbons and water (as will be shown below) by late transition metal ions is suppressed compared with this process for early transition metal ions.[13] The $FeO^+ + D_2$ reaction allows this process to be studied in reverse. In addition, comparison of these results with those for reaction of the bare metal ion ($Fe^+ + D_2$)[9] enable an assessment of the influence of the oxo ligand on reactivity. Previous work involving reaction of FeO^+ with small hydrocarbons[5,6] at thermal energies has shown that it is more reactive than its naked metal counterpart Fe^+, although the electronic state of the Fe^+ reactant has not been considered in these studies. Here, we are able to show that FeO^+ and $Fe^+(a^4F)$ have comparable reactivities that greatly exceed that for $Fe^+(a^6D)$.

One requisite to understanding iron–hydroxide formation is a definitive value for the Fe^+–OH bond energy. Several values for $D(Fe^+–OH)$ have been reported including 3.34 ± 0.26 and 3.17 ± 0.13 eV by Cassady and Freiser,[14] 3.30 ± 0.20 eV by Murad,[15] and 3.70 ± 0.13 eV by Magnera, David, and Michl.[16] In experiments designed to measure this bond energy, which will be published separately,[8] we have measured the endothermicity associated with formation of $FeOH^+$ from the bimolecular reaction of Fe^+ with methanol and from threshold collisional activation of Fe^+–CH_3OH and H_3C–Fe^+–OH to form $FeOH^+ + CH_3$. These three measurements are in agreement with one another and lead to the value $D(Fe^+–OH) = 3.79 \pm 0.12$ eV (Table 1, where we assume that $D(Fe^+–OD) = D(Fe^+–OH)$, a reasonable equation, as discussed elsewhere[17,18]). This value is in good agreement with the value obtained by Magnera et al.[16] and is used throughout this work.

While this study was in progress, Schröder, Fiedler, Ryan, and Schwarz (SFRS) reported a Fourier transform ion cyclotron resonance (FTICR) study of the $FeO^+ + H_2$, HD, and D_2 reactions.[19] They noted that, on the basis of previous work from our laboratory concerning the reactions of ScO^+, TiO^+, and VO^+ with D_2,[17] one might expect that FeO^+ should react efficiently with H_2 or D_2 to form water. Instead, they find that the reaction is inefficient but can be driven by kinetic energy. We confirm these results while providing more quantitative information by examining the kinetic energy dependence of this reaction and its reverse in more detail. Comparison of these results to parallel results for cobalt[20] is also enlightening.

Experimental Section

General. Complete descriptions of the apparatus and experimental procedures are given elsewhere.[21,22] Ions are produced in a surface ionization (SI) source and in a dc discharge/flow tube (FT) source described below. The ions are extracted from the source, accelerated, and focused into a magnetic sector momentum analyzer for mass analysis. Mass-selected ions are slowed to a desired kinetic energy and focused into a radio-frequency (rf) octopole ion guide that radially traps the ions. As discussed elsewhere,[21,23] the octopole is superior to the rf-only quadrupole for reactivity studies and can provide efficient collection of products over a 4π solid angle and a wide mass range if operated

† Present address: Department of Chemistry, Northwestern University, 2145 Sheridan, Evanston, IL 60208.

* Abstract published in *Advance ACS Abstracts*, June 1, 1994.

0022-3654/94/2098-6522$04.50/0

judiciously. Such safe operating conditions are outlined in detail by Gerlich,[23] and our operating conditions fall well within these safe conditions for the range of masses included in this study. The octopole passes through a static gas cell containing the neutral reactant. Gas pressures in the cell are kept low (between ~0.05 and 0.30 mTorr in the case of water and below 0.50 mTorr for D_2) so that multiple ion–molecule collisions are improbable. Product and unreacted beam ions are contained in the guide until they drift out of the gas cell where they are focused into a quadrupole mass filter for mass analysis and then detected. Ion intensities are converted to absolute cross sections as described previously.[21] Uncertainties in cross sections are estimated to be ±20%.

Laboratory energies are converted to center-of-mass (CM) frame energies by $E_{CM} = E_{lab}\, m/(M + m)$ where M and m are the ion and neutral reactant masses, respectively. Below ~0.3 eV lab, energies are corrected for truncation of the ion beam energy distribution as described previously.[21] Uncertainties in the absolute energy scale are ±0.05 eV lab. Two effects broaden the data: the ion energy spread, which is independent of energy and has a full width at half-maximum (fwhm) of ~0.7 eV lab for the SI source and ~0.4 eV lab for the FT studies, and thermal motion of the neutral gas, which has a width of $0.46E_{CM}^{1/2}$ for reaction of Fe^+ with D_2O and $0.52E_{CM}^{1/2}$ for reaction of FeO^+ with D_2.[24]

Ion Sources. In the SI source, $Fe(CO)_5$ (Alfa, 99.5%) vapor is directed toward a resistively heated rhenium filament, where it decomposes, and the resulting metal atoms are ionized. It is assumed that ions produced by SI equilibrate at the filament temperature and the state populations are governed by a Maxwell-Boltzmann distribution. The validity of this assumption has been discussed previously[25] and has recently been confirmed for Co^+ by van Koppen et al.[26] Also, resonant two-phonon ionization (R2PI) experiments by Weisshaar and co-workers[11,12] involving the quartet and sextet states of Fe^+ are consistent with our assumption of a Boltzmann distribution of these states for our SI source. The temperature of the SI filament used in these experiments is 2300 ± 100 K. Under these conditions, the Fe^+ beam comprises mostly a^6D ground-state ions, 78.3 ± 1.1% with a J-averaged electronic energy (E_{el}) of 0.052 eV, and a^4F first excited state ions, 21.3 ± 0.9% (E_{el} = 0.300 eV). Less than 0.5% of the beam is in higher electronic states of Fe^+.

The FT source has been described in detail previously.[22,27] Fe^+ is generated in a dc discharge by 1.5–3.0-keV Ar ion impact on a cylindrical rod (1.25 cm in diameter and ~2.5 cm in length) made of carbon steel. The ions are then swept down a meter long flow tube by He and Ar flow gases maintained at pressures of ~0.50 and ~0.05 Torr, respectively. We calculate that under these conditions the ions undergo ~10^5 collisions with He and ~10^4 collisions with Ar before exiting the flow tube. The Fe^+ beam produced in this manner is substantially colder than the beam produced by SI, a result that is discussed in more detail in the Results section.

FeO^+ was produced in the flow tube by interaction of the bare metal ions with either N_2O or NO_2. In the former case, N_2O is injected into the source region of the instrument at pressures less than 1 mTorr and FeO^+ is formed in the energetic plasma near the discharge region of the source. The overall reaction of Fe^+ with N_2O, exothermic by 1.80 ± 0.06 eV[28] has been discussed previously.[29] FeO^+ can also be formed from interaction of Fe^+ with NO_2 that is introduced ~50 cm downstream. This reaction is exothermic by only 0.35 ± 0.06 eV[28] and therefore limits the internal energy of the FeO^+ produced. In either case, the FeO^+ ions produced should be thermalized with respect to electronic, vibrational, and rotational states from the many collisions with the carrier gasses. This is consistent with the observation that results of these experiments for FeO^+ produced by reaction with both N_2O and NO_2 are identical within experimental uncertainty. Collision-induced dissociation (CID) of FeO^+ with Xe indicates that the ions are not internally excited.[30] Further, no changes in reactivity of the FeO^+ beam were observed when H_2 or O_2 was added to the flow tube to effect additional cooling. We assume that these ions have equilibrated to the 300 K temperature of the flow gasses. Previous work from this laboratory[27,31–36] has shown that this assumption is reasonable.

Thermochemical Analysis. Previous work[37,38] has shown that cross sections for endothermic reactions can be analyzed by using eq 1

$$\sigma(E) = \sigma_0(E - E_0 + E_{vib} + E_{rot})^n/E \qquad (1)$$

where σ_0 is a scaling factor, E is the relative kinetic energy, n is an adjustable parameter, and E_0 is the 0 K threshold for reaction of ground electronic, vibrational, and rotational state reactants. In this study, E_{vib} represents the average reactant vibrational energy (<0.001 eV for both systems) and E_{rot} is the total reactant rotational energy ($3kT/2$ = 0.039 eV and $2kT$ = 0.053 eV for the $Fe^+ + D_2O$ and $FeO^+ + D_2$ systems, respectively) at 305 K (the nominal temperature of the octopole). After convoluting the model over the neutral and ion kinetic energy distributions as described previously,[21] the σ_0, n, and E_0 parameters are optimized by using a nonlinear least-squares analysis to give the best fit to the data. Error limits of E_0 are calculated from the range of threshold values for different data sets over a range of n values and the error in the absolute energy scale.

A modified form of eq 1 accounts for depletion of the product ion at higher energies. This model, described in detail previously,[39] depends on the energy where a dissociation channel or a competing reaction can begin. The use of this model is required for analysis of the $FeOD^+$ cross sections measured for both the $Fe^+ + D_2O$ and $FeO^+ + D_2$ reaction systems, because the shapes of these cross sections are heavily influenced by competition with other reaction channels as discussed below. In addition, the use of this modified form allows the data to be analyzed over a much broader energy region, thereby defining the optimum parameters of eq 1 more accurately.

Results

$Fe^+ + D_2O$. Three ionic products, formed in reactions 2–4 (where the indicated thermochemistry is calculated for ground-state species from information in Table 1),are observed in the

$$Fe^+ + D_2O \rightarrow FeD^+ + OD \quad -3.04 \pm 0.06\ eV \qquad (2)$$

$$\rightarrow FeOD^+ + D \quad -1.42 \pm 0.12\ eV \qquad (3)$$

$$\rightarrow FeOD_2^+ + 1.33 \pm 0.05\ eV \qquad (4)$$

reaction of Fe^+ with D_2O. The cross sections for reactions 2–4, when Fe^+ is produced in the SI and FT sources, are shown in Figure 1. No evidence of FeO^+ formation was observed in this study, indicating that $\sigma(FeO^+) < 1 \times 10^{-19}$ cm^2 for the SI data and $< 5 \times 10^{-20}$ cm^2 for the FT data. The failure to observe this product is not due to thermodynamic constraints, because the thermodynamic onset for dehydrogenation of water by Fe^+ is 1.64 ± 0.06 eV, calculated from values in Table 1, within the energy range studied here. The cross sections for reaction 4 depend linearly on the pressure of D_2O in the reaction cell (which is slightly different for the SI and FT data sets). This indicates that $FeOD_2^+$ is formed by secondary collisions with D_2O that stabilize this adduct. Reactions 2 and 3 result from single-collision events, as verified by pressure studies, and are clearly endothermic. The $FeOD^+$ cross sections exhibit two features. The one at lower kinetic energy peaks near the onset of reaction 2, well below the energy needed for this product to dissociate to $Fe^+ + OD$, 5.212

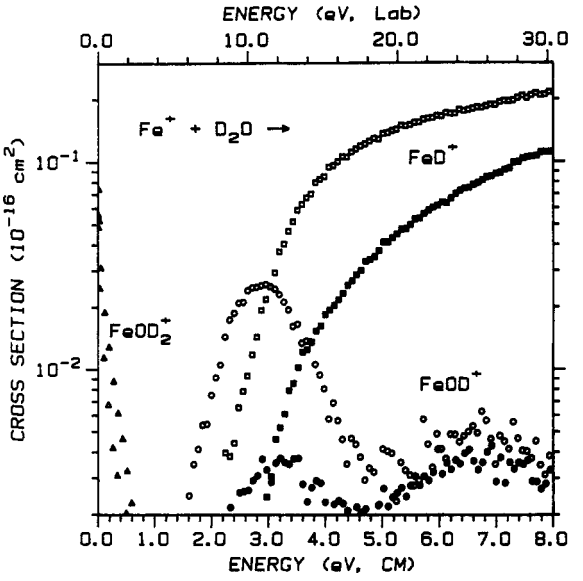

Figure 1. Variation of product cross sections for reaction of Fe^+ produced in the surface ionization (SI, open symbols, $P(D_2O)$ = 0.36 mTorr) and flow tube (FT, closed symbols, $P(D_2O)$ = 0.41 mTorr) sources with D_2O to form FeD^+ + OD (squares), $FeOD^+$ + D (circles), and $FeOD_2^+$ (triangles) as a function of kinetic energy in the center-of-mass frame (lower scale) and the laboratory frame (upper scale).

TABLE 1: Thermochemistry at 0 K

bond	D_0, eV	bond	D_0, eV	bond	D_0, eV
D–D	4.556[a]	Fe^+–D	2.17(0.06)[b]	Fe^+–OD	3.79(0.12)[e,f]
O–D	4.454(0.002)[a]	Fe^+–O	3.47(0.06)[c,d]	Fe^+–OD_2	1.33(0.05)[f,g]
DO–D	5.212(0.002)[a]				

[a] Calculated from heats of formation given by: Gurvich, L. V.; et al. *Thermodynamic Properties of Individual Substances*; Hemisphere: New York, 1989; Vol. 1, Part 2. [b] Value derived from $D_0(Fe^+–H)$ = 2.12 ± 0.06 eV by adjusting for the differences in zero-point energies of FeH^+ and FeD^+, 0.049 eV (ref 9). [c] Reference 42 and Loh, S. K.; Fisher, E. R.; Lian, L.; Schultz, R. H.; Armentrout, P. B. *J. Phys. Chem.* **1989**, *93*, 3159. [d] Reevaluated in ref 43. [e] Reference 8. [f] Deuteriation is assumed not to influence these bond energies. [g] Reference 55.

eV (Table 1). This indicates that reactions 2 and 3 compete directly. At high energies, formation of FeD^+ dominates the reactivity as is typically observed in reactions of atomic metal atoms with hydrogen-containing polyatomic molecules.[40]

More insight into the origin of the two features in $\sigma(FeOD^+)$ can be gained by comparing the cross sections for the $Fe^+ + D_2O$ reaction when the Fe^+ beam is produced in the SI and FT sources (Figure 1). The qualitative features of the FT data are similar to the SI data except that the low-energy portion of $\sigma(FeOD^+,FT)$ is a factor of ~8 smaller, while the high-energy portion is largely unchanged. The decrease at low energies is consistent with a smaller population of excited $Fe^+(a^4F)$ ions in the FT beam. Thus, between ~1.5 and ~5 eV, $\sigma(FeOD^+)$ is dominated by reaction of $Fe^+(a^4F)$, while above ~5 eV, the cross section is dominated by reaction of ground-state $Fe^+(a^6D)$ ions because its population in the SI and FT beams changes little.[41] We determine the population of the $Fe^+(a^4F)$ ions in the FT beam by comparing the magnitudes of $\sigma(FeOD^+,FT)$ and $\sigma(FeOD^+,SI)$ in the low-energy region below 4.0 eV. Given that the a^4F state comprises 21.3 ± 0.9% of the SI beam, this comparison establishes that the FT beam comprises 2.8 ± 0.6% of the a^4F state.

Although the changes observed for the FeD^+ data channel between the SI and FT data are not as striking as observed for the $FeOD^+$ data channel, the FeD^+ cross sections clearly differ (Figure 1). $\sigma(FeD^+,SI)$ rises more rapidly with increasing energy and has a lower apparent threshold than does $\sigma(FeD^+,FT)$. Thus, the threshold region of $\sigma(FeD^+,SI)$ is dominated by reaction of

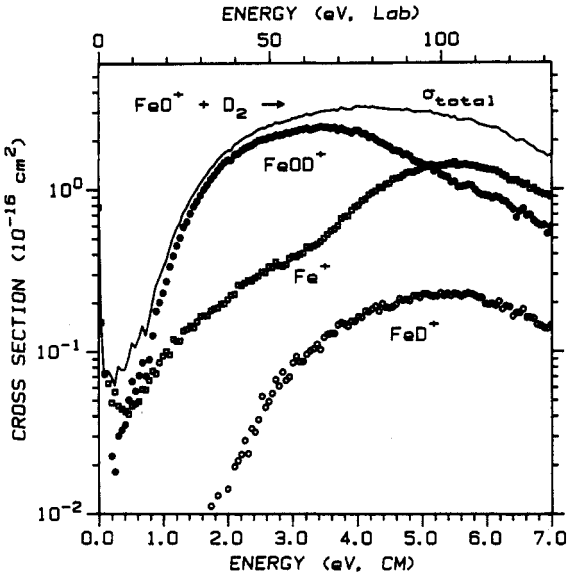

Figure 2. Variation of product cross sections for reaction of FeO^+ with D_2 to form $Fe^+ + D_2O$ (open squares), $FeOD^+ + D$ (solid circles), and $FeD^+ + OD$ (open circles) as a function of kinetic energy in the center-of-mass frame (lower scale) and the laboratory frame (upper scale).

$Fe^+(a^4F)$ ions, which are substantially more reactive than $Fe^+(a^6D)$ ions. This comparison is done more quantitatively below.

$FeO^+ + D_2$. Three ionic products corresponding to reactions 5–7 (where the indicated thermochemistry is calculated for ground-state species from the information in Table 1), are observed in the reaction of FeO^+ with D_2. The cross sections for these reactions are shown in Figure 2. In all cases, it was verified by pressure-dependent studies that the cross sections shown result from single-collision events. The Fe^+ cross section (reactions 5) displays a rather complicated behavior. Below ~0.5 eV, $\sigma(Fe^+)$ increases as energy is decreased to as low an energy as we can measure, indicating that this portion of the cross section is due to an exothermic reaction. This means that Fe^+ formation is accompanied by loss of the stable D_2O molecule (reaction 5a). Above ~0.5 eV, $\sigma(Fe^+)$ increases slowly until ~3.5 eV, where the cross section begins to rise more rapidly. The energetics associated with this latter increase are consistent with either a collision-induced dissociation process to form an oxygen atom and D_2 as the accompanying neutral products (reaction 5b) or formation of OD + D as the neutral products (reaction 5c). The difference between the energies of these two processes is too small for us to unambiguously distinguish which reaction is responsible for the increase in the cross section. The endothermic portion of the Fe^+ cross section below 3.5 eV must still correspond to elimination of water because this is the only process that is thermodynamically feasible. Thus, there are two distinct pathways for reaction 5a.

$$FeO^+ + D_2 \rightarrow Fe^+ + D_2O + 1.64 \pm 0.06\ eV \quad (5a)$$

$$\rightarrow Fe^+ + O + D_2 - 3.47 \pm 0.06\ eV \quad (5b)$$

$$\rightarrow Fe^+ + OD + D - 3.57 \pm 0.06\ eV \quad (5c)$$

$$\rightarrow FeD^+ + OD - 1.40 \pm 0.09\ eV \quad (6)$$

$$\rightarrow FeOD^+ + D + 0.22 \pm 0.13\ eV \quad (7)$$

The thermochemistry in Table 1 indicates that formation of $FeOD^+$ in reaction 7 is exothermic; however, the cross section for $FeOD^+$ formation shown in Figure 2 clearly exhibits endothermic behavior. This immediately suggests that this process proceeds over a reaction barrier, but alternate explanations involve excited states or isomers of the $FeOD^+$ species, as discussed below. The $FeOD^+$ cross section peaks near 3.5 eV, consistent with the thermodynamic thresholds for reaction 5b, CID of FeO^+, and reaction 5c, cleavage of the Fe^+–OD bond. This behavior differs

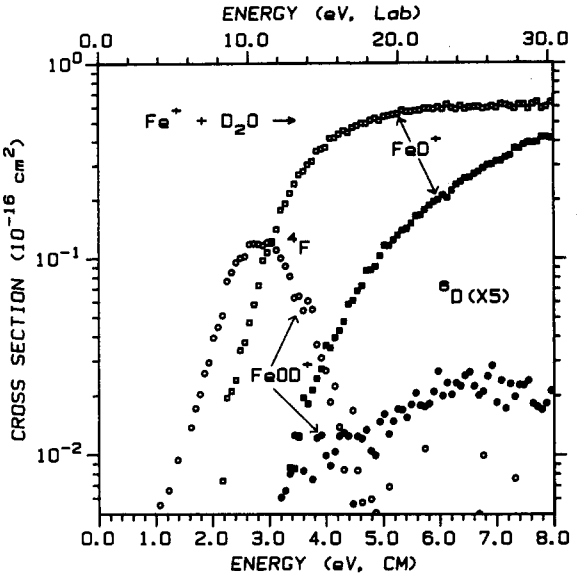

Figure 3. State-specific cross sections for the reaction of water with Fe^+ as a function of translational energy in the laboratory (upper axis) and center-of-mass frame (lower axis). Solid and open symbols show results for $Fe^+(a^6D)$ (multiplied by five) and $Fe^+(a^4F)$, respectively, derived as discussed in the text. In both cases, squares represent the FeD^+ product and circles represent the $FeOD^+$ product.

somewhat from that observed for reaction of ScO^+, TiO^+, and VO^+ with D_2,[17] where the MOD^+ cross sections all peak at about 4.5 eV due to dissociation to form $MO^+ + D + D$. For these three metals, this is the lowest energy dissociation pathway for MOD^+ because the metal–oxide bond energies are about twice that of FeO^+,[42,43] making the pathways analogous to reactions 5b and 5c much higher in energy.

The results shown in Figure 2 are very similar in magnitude and energy dependence to those for the reaction of CoO^+ with D_2 with the exception of one detail:[20] there is no exothermic feature observed at the lowest energies for formation of Co^+ even though production of $Co^+ + D_2O$ is exothermic. In the cobalt system, we concluded that there was a common barrier to the reaction that formed $CoOD^+ + D$ and $Co^+ + D_2O$.

Data Analysis

State-Specific Cross Sections for $Fe^+(a^6D)$ and $Fe^+(a^4F)$ + D_2O. The SI and FT cross sections displayed in Figure 1 can be used to derive cross sections specific to reaction of $Fe^+(a^6D)$ and $Fe^+(a^4F)$. These results are shown in Figure 3 and are obtained as follows. Because $\sigma(FeD^+,FT)$ is due to the reactivity of nearly 100% $Fe^+(a^6D)$, this cross section can be scaled by its fractional population in the SI beam (0.78) and subtracted from the SI data in order to yield a cross section due almost exclusively to reaction of $Fe^+(a^4F)$ ions. The absolute cross section for this state is obtained by dividing this cross section by its fractional population in the SI beam, 0.21. The final cross section for $FeD^+(a^6D)$ is obtained by scaling $\sigma(FeD^+,a^4F)$ by its 2.8% population in the FT beam, subtracting this scaled cross section from $\sigma(FeD^+,FT)$, and readjusting the absolute magnitude.

State-specific cross sections for the $FeOD^+$ data channel can be derived in a similar manner, only for this channel we have fit the first feature of the SI data using eq 1 and the E_0 and n parameters given in Table 2 in order to obtain a cross section shape that is representative of $\sigma(FeOD^+,a^4F)$. This fit is then scaled to the low-energy feature in the FT data and subtracted in order to obtain $\sigma(FeOD^+,a^6D)$. $\sigma(FeOD^+,a^4F)$ is then obtained by scaling $\sigma(FeOD^+,a^6D)$ by its population in the SI beam, subtracting this scaled cross section from $\sigma(FeOD^+,SI)$, and readjusting the magnitude according to the population, as was done for the FeD^+ channel. Alternatively, $\sigma(FeOD^+,a^6D)$ can be determined by subtracting the fit to the a^4F cross section from the SI data and then scaling the remaining high-energy portion of the cross section by the inverse of 0.78. This yields a cross section that is a factor of ~1.5 times larger than $\sigma(FeOD^+,a^6D)$ determined from the FT data (a factor that is actually apparent in the raw data shown in Figure 1). This factor is a conservative estimate of the absolute uncertainty of these state-specific cross sections.

TABLE 2: Summary of Parameters for Eq 1

reactants	products	E_0, eV	σ_0	n
$Fe^+(a^6D) + D_2O$	$FeD^+ + OD$	≡3.04[a]	0.023	2.1
$Fe^+(a^4F) + D_2O$	$FeD^+ + OD$	≡2.76[a]	1.21	1.0
$Fe^+(a^6D) + D_2O$	$FeOD^+ + D$[b]	1.66(0.22)	0.0008(0.0009)	2.8(0.9)
$Fe^+(a^4F) + D_2O$	$FeOD^+ + D$	1.38(0.22)	0.17(0.11)	2.8(0.9)
$FeO^+ + D_2$	$Fe^+ + D_2O$[b]	0.5(0.2)	0.16(0.02)	1.9(0.1)
$FeO^+ + D_2$	$Fe^+ + O + D_2$[b]	3.53(0.16)	2.24(0.46)	1.2(0.2)
$FeO^+ + D_2$	$FeD^+ + OD$	1.79(0.07)	0.15(0.03)	1.7(0.2)
$FeO^+ + D_2$	$FeOD^+ + D$	0.62(0.08)	1.25(0.23)	2.3(0.3)

[a] These fits use thresholds that are held to the thermodynamic values calculated from the information in Table 1. [b] See text for discussion of these fitting parameters.

One test of this derivation is to compare the $Fe^+(a^4F) + D_2O$ cross sections with those for $Co^+(a^3F) + D_2O$.[20] Previous work[44] indicates that $Fe^+(a^4F)$ and $Co^+(a^3F)$ react similarly because they have comparable electron configurations, $3d^7$ and $3d^8$, respectively. This comparison finds that the Co^+ and $Fe^+(a^4F)$ cross sections are indeed similar in magnitude, energy dependence, and the failure to observe the $MO^+ + D_2$ product channel. We also note that the a^6D and a^4F cross sections display drastic differences in their kinetic energy dependence. For both reaction channels, the cross sections for the a^4F state rise more rapidly with energy than the cross sections for reaction of $Fe^+(a^6D)$. This is similar to the state-specific behavior observed for reaction of Fe^+ with H_2 and alkanes.[9,10]

Threshold Analyses—$Fe^+ + D_2O$. The state-specific cross sections derived above are analyzed by eq 1 and the parameters given in Table 2. For the FeD^+ channel, the thermochemistry listed in Table 1 yields thresholds for reaction of the a^6D and a^4F states of 3.04 ± 0.06 and 2.76 ± 0.07 eV, respectively (given an average electronic energy of 0.28 eV for the a^4F state at 2300 K). Use of these thresholds in eq 1 allows the cross sections to be reproduced very well with the other parameters given in Table 2. Comparison of the σ_0 values for these fits shows that $Fe^+(a^4F)$ is more reactive than $Fe^+(a^6D)$ by a factor of ~50. This result is similar to the relative reactivity difference of ~70 observed for reaction of $Fe^+(a^6D)$ and $Fe^+(a^4F)$ with H_2 to form $FeH^+ + H$.[9]

Analysis of the threshold for the $Fe^+(a^4F)$ state reacting to form $FeOD^+$ with eq 1 and the parameters given in Table 2 gives $E_0 = 1.38 \pm 0.22$ eV. This value is within experimental error of the 1.14 ± 0.12 eV threshold calculated for reaction of $Fe^+(a^4F)$. Although it is possible that there is a small reaction barrier in this system, we hesitate to conclude this because the SI and FT cross sections used to derive $\sigma(FeOD^+,a^4F)$ are extremely small, and therefore any slow rise of the data near the threshold for these cross sections is difficult to observe. In our recent study of the reaction of Co^+ with D_2O,[20] the threshold for formation of $CoOD^+$ was observed to rise slowly from its thermodynamic threshold, and we anticipate similar behavior here.

Analysis of the $FeOD^+$ data channel for reaction of $Fe^+(a^6D)$ is even more ambiguous than for the $Fe^+(a^4F)$ state because the cross section is much smaller, with a maximum magnitude of only ~0.004 Å^2. Although the threshold obtained from these data may be inconclusive concerning thermochemistry, it is useful to analyze these data in order to obtain a value for σ_0 so that the magnitude of the reactivity differences between the a^6D and a^4F states can be determined. We have analyzed the data by constraining the threshold of eq 1 to values that are 0.28 eV higher than each of the fits used in determining the 1.38 ● 0.22

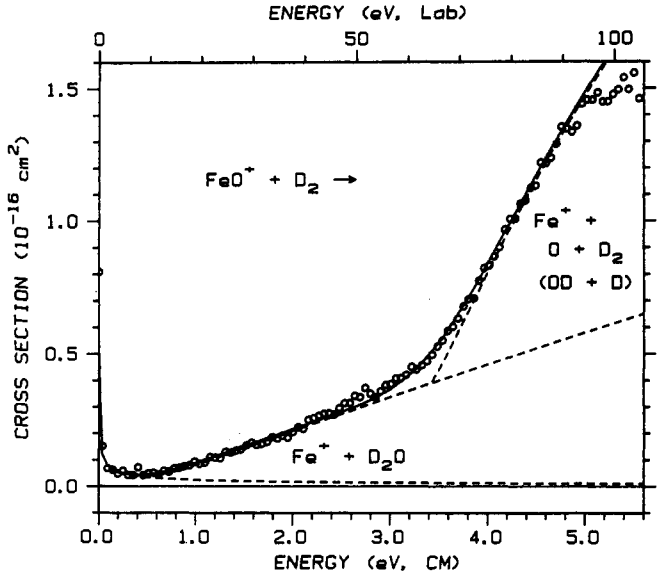

Figure 4. Kinetic energy dependence of $\sigma(Fe^+)$ formed by reaction of FeO^+ with D_2 as a function of translational energy in the laboratory frame (upper axis) and center-of-mass frame (lower axis). The dashed lines indicate the three components believed to comprise the experimental cross section, as detailed in the text. The full line is the sum of these three model components convoluted over the experimental kientic energy distributions.

eV threshold for the $\sigma(FeOD^+,{}^4F)$. (The parameter n is also constrained to the values used for each of the fits for the ^4F cross section.) Comparison of the values of σ_0 necessary to represent the a^4F and a^6D cross sections as analyzed by this method suggests that the former state is more reactive by a factor of ~200.

Threshold Analyses—$FeO^+ + D_2$. The cross sections for processes 6 and 7 in the reaction of FeO^+ with D_2 can also be analyzed by eq 1, and the optimized parameters are given in Table 2. For the FeD^+ cross section, this analysis gives a threshold of 1.79 ± 0.07 eV, although the data can also be reproduced by using the thermodynamic threshold of 1.40 eV and a slightly higher value of n (=2.2 ± 0.1). These results are most consistent with a reaction for which there is no barrier in excess of the reaction endothermicity but that is inefficient at threshold, probably due to competition with the more probable reactions 5 and 7. It also helps verify that the FeO^+ beam is thermalized, because the threshold measured for FeD^+ would be lower than the thermodynamic threshold if a significant portion of the FeO^+ beam were in excited vibrational or electronic states.

Analysis of $\sigma(FeOD^+)$ with eq 1 and the parameters given in Table 2 gives a threshold of 0.62 ± 0.08 eV. Because reaction 7 is exothermic, this threshold must correspond either to formation of an isomer or excited state of $FeOD^+$ or to a barrier along the potential energy surface.

As mentioned above, the thermochemistry given in Table 1 can be used to calculate that reaction 5a is exothermic by 1.64 ± 0.06 eV, consistent with the small exothermic portion of the cross section shown in Figure 2. The endothermic portion of these data below $D(Fe^+–O)$ = 3.47 ± 0.06 eV must also be due to formation of $Fe^+ + D_2O$, but in a process that involves a reaction barrier. To gain a feeling for the magnitude of this barrier, we have modeled the data as shown in Figure 4. The exothermic reactivity is accounted for by scaling the Langevin–Gioumousis–Stevenson[45] model collision cross section by a factor of 0.0017 ± 0.0001. The low-energy endothermic feature can be modeled by using a threshold of 0.5 eV and the parameters given in Table 2. The high-energy feature due to either reaction 5b or 5c is represented by eq 1 with a threshold of 3.53 ± 0.16 eV, consistent with the thermodynamic thresholds. We note that if other models for accounting for the exothermic and CID portions of this cross section are used, then slightly higher or lower values of the threshold for the reaction barrier are obtained. We conservatively estimate the uncertainty associated with the threshold for this 0.5 eV barrier to be ~0.2 eV.

Comparison to Previous Results for $FeO^+ + D_2$. In 1981, Kappes and Staley[46] reported that FeO^+ generated by reaction of Fe^+ with N_2O reacts rapidly with H_2 to give $FeOH^+$. SFRS[19] note that this exothermic reactivity disappears if the FeO^+ ions are thermalized first. The present results confirm that formation of $FeOH^+$ in reaction 7 is negligible at thermal energies. In the FTICR study of SFRS, the kinetic energy dependence of the reaction of FeO^+ with H_2 was examined, although the absolute energy scale cannot be determined with any confidence. The results obtained by SFRS are consistent with the present results shown in Figure 2 if the laboratory energy scale of SFRS is divided by about 10 to yield an effective center-of-mass energy scale. The qualitative energetic behavior of all three cross sections is similar to the present results, although relatively more Fe^+ is observed by SFRS. This appears to be due primarily to a much more efficient exothermic pathway than is observed here. The present results can be converted[21] to a thermal rate constant for Fe^+ production of 1.5×10^{-12} cm^3/s, while SFRS report 1.1×10^{-11} cm^3/s. The most obvious explanation for this discrepancy is that the cooling of the FeO^+ is incomplete in the FTICR experiment, where it is difficult to achieve the large number of collisions afforded by the flow tube source source used here. The key observation, however, is that SFRS observe the same complicated behavior that is observed in the present experiment. This helps confirm that this behavior is intrinsic to the system, rather than being an artifact of the experimental conditions in either study.

Discussion

Potential Energy Barriers or Isomers. One possible explanation for the elevated thresholds observed in these systems for formation of $FeOD^+$ is that an O–Fe^+–D isomer is formed. Two considerations make this unlikely. The first can be seen by assuming that the thresholds for reactions 3 and 7 (Table 2) correspond to formation of O–Fe^+–D. These thresholds then lead to the bond energies, $D_0(OFe^+–D)$ = 4.54 ± 0.23 and 3.94 ± 0.10 eV, respectively. These values are much larger than the diatomic metal–deuteride bond energy, $D_0(Fe^+–D)$ = 2.17 ± 0.06 eV, and are much closer to $D_0(O–D)$ = 4.454 eV (Table 1). For diatomic first-row transition metal–hydride cations, it has been shown that the *strongest* M^+–H bond energy is about 2.6 eV.[47-49] It seems unlikely that the oxo ligand could enhance this maximum bond energy by over 50%.

The second consideration is that reaction 5, elimination of water, shows clear evidence for a reaction barrier in the endothermic portion of this cross section (Figure 2). The fact that this portion has a threshold similar to that observed for reaction 7 can be explained readily if these two reactions proceed via a common transition state, located about 0.6 eV above the energy of the $FeO^+ + D_2$ reactants.

$Fe^+ + D_2O$ Reaction Mechanism. Two obvious mechanisms exist for formation of FeD^+ and $FeOD^+$ in the reaction of Fe^+ with D_2O: by insertion to form D–Fe^+–OD or by direct ligand abstraction of the D atom or OD group by Fe^+. Oxidative addition of O–D (or any σ bond) to an iron center to form D–Fe^+–OD is achieved by donation of electrons in σ–bonding orbitals into the empty 4s orbital of the metal and back-donation of the metal $3d\pi$ electrons into the σ^*-antibonding orbital.[50] This increases the electron density between the metal and molecular fragments while lengthening the O–D bond. If the resulting D–Fe^+–OD intermediate is bound by covalent Fe–D and Fe–OD bonds, then there will be five electrons left in four, closely spaced nonbonding orbitals, and this species should have a quartet spin ground state. SFRS suggest that this species should have a sextet spin, but this requires promotion of one of the paired nonbonding electrons into an antibonding orbital (or into an orbital with extensive

4p-like character). We note that the analogous $Fe(CH_3)_2^+$ species has been calculated to have a quartet spin ground state by Rosi et al.,[51] although it is possible that the back-bonding interactions with the hydroxide ligand help stabilize the sextet states. [After completion of this work and submission of this paper, we learned that Fiedler et al.[52] have calculated that this intermediate has a quartet ground state. Further, this theoretical work confirms many aspects of the potential energy surfaces developed below.]

Clearly, a D–Fe^+–OD insertion intermediate explains the strong competition observed between formation of $FeOD^+$ and FeD^+ in the reaction of $Fe^+(^4F)$ (Figure 3) because breaking the Fe–D bond forms $FeOD^+$, while breaking the Fe–OD bond produces FeD^+. Further, because formation of such a quartet intermediate is spin-forbidden from the $Fe^+(a^6D)$ ground state, the inefficiency of the reactivity of this state relative to the a^4F state is easily explained. Indeed, the observation that direct competition between reactions 2 and 3 is not obvious for reaction of $Fe^+(a^6D)$. (Figure 3) suggests that $Fe^+(a^6D)$ may react primarily though a direct process that forms FeD^+ preferentially. The direct reaction is spin-allowed from both the a^6D and a^4F states of Fe^+ because the final products are $FeD^+(^5\Delta) + OD(^2\Pi)$ and $FeOD^+(^5A) + D(^2S)$.[53] These state-specific results are not easily explained by a ground-state intermediate having sextet spin, although this is still a possibility as long as the barriers to elimination of D_2O and D_2 from this intermediate are large. This seems likely for reasons discussed further below.

For both the a^6D and the a^4F states, formation of FeD^+ dominates at higher energies. As noted above, this is a typical result for production of metal–hydride ions from the reaction of bare metal ions with H-containing polyatomic molecules. An important consideration in understanding this result is that angular momentum constraints favor metal–hydride formation over formation of the more massive metal–ligand product. These constraints have been discussed in detail previously.[25,54] It is also worth noting that as energy is increased, the FeD^+ cross sections for reaction of both states tend to converge. This can be seen by examining Figure 3. At ~4.0 eV, the a^4F cross section is larger than the a^6D cross section by a factor of ~60, while at 8 eV, this factor is less than 4. This can be explained by realizing that a direct reaction mechanism can be utilized by both states at high energies.

$Fe^+ + D_2O$ Potential Energy Surfaces. Additional insight into these reactions can be obtained by considering the qualitative potential energy surfaces that must be involved. The initial interactions of $Fe^+(a^6D)$ and $Fe^+(a^4F)$ with D_2O are attractive due to long-range ion–dipole interactions. The depth of the Fe^+–OD_2 well is taken to equal the Fe^+–OH_2 bond energy (Table 1) obtained from collision-induced dissociation studies of Fe^+–OH_2 conducted in our laboratory.[55] This value is in good agreement with other measurements of Magnera, David, and Michl[16] and of Marinelli and Squires[56] and calculations by Rosi and Bauschlicher.[57] The calculations also indicate that $FeOH_2^+$ has a $^6A_1$ ground state and a $^4A_1$ first excited state that lies only 0.19 eV higher in energy, although the splitting could be as small as 0.03 eV.[58] These various conclusions are indicated in Figure 5.

As the Fe^+ ion approaches D_2O close enough to insert, the qualitative potential energy surfaces can be understood by using molecular orbital arguments, as discussed in previous work on the reactivities of $Fe^+(a^6D,4s3d^6)$ and $Fe^+(a^4F,3d^7)$.[9,10] The different electron configurations of the two states of Fe^+ lead to distinctly different potential energy surfaces. The occupied 4s orbital of the a^6D state leads to repulsive surfaces, and hence its reactivity is inefficient and shifted to higher energies (Figure 3). Because the a^4F state has an empty 4s orbital, the potential energy surfaces are more attractive, and this state can insert into the DO–D bond along a spin allowed pathway (Figure 5). The energy of the D–Fe^+–OD intermediate is estimated by assuming that $D(DFe^+–OD) \approx D(H_3CFe^+–OH) \approx 2.5$ eV.[8] This estimate puts

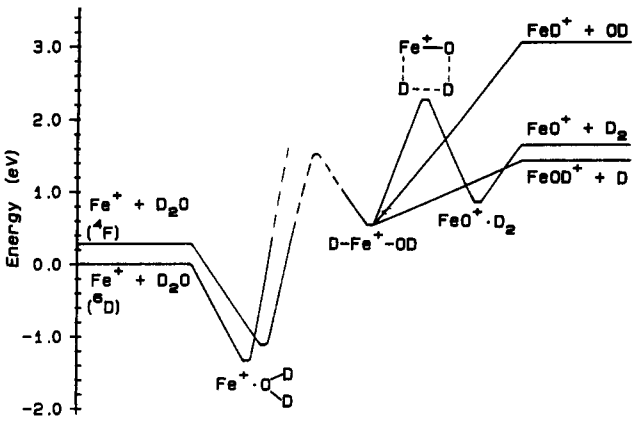

Figure 5. Semiquantitative potential energy diagram for the $[FeD_2O]^+$ system. Details of the electronic character of the $FeO^+ + D_2$ channel are not included. Dashed lines indicate a region of the potential energy surface where there is no quantitative experimental information.

the intermediate at an energy of 0.54 eV above the ground-state reactants. The energetics for the transition state associated with this insertion process are examined below.

Because there is a crossing between the quartet and sextet surfaces in the entrance channel, as shown in Figure 5, there is the possibility of transferring from one surface to the other due to spin–orbit interactions. The observation that $Fe^+(^6D)$ forms $FeOD^+$ indicates that this transfer is probably occurring but the observation that $Fe^+(^4F)$ undergoes this reaction about 200 times more readily than $Fe^+(^6D)$ suggests that the surface mixing is fairly inefficient.

$FeO^+ + D_2$ Mechanism and Potential Energy Surfaces. Irikura and Beauchamp[59] and we[17] have previously discussed three possible mechanisms for the activation of D_2 by a MO^+ ion: oxidative addition of the D–D bond to the metal end of the molecule to form D_2MO^+, oxidative addition of the D–D bond to the oxygen end of the MO^+ molecule to form M^+–OD_2, or addition across the M–O bond via a four-centered intermediate to form D–M^+–OD. These various pathways have been discussed in detail in our paper on the activation of D_2 by ScO^+, TiO^+, and VO^+.[17] For reasons directly analogous to this discussion, we find that the most likely mechanism here is addition of D_2 across the FeO^+ bond to form the D–Fe^+–OD intermediate also invoked for the bare metal reaction with D_2O. SFRS reach the same conclusion by using the same analysis.

If the reaction of FeO^+ with D_2 does occur by formation of the D–Fe^+–OD intermediate, this channel must appear on the potential energy surface of Figure 5. The key experimental observation is that both reactions 5a (to form $Fe^+ + D_2O$) and 6 (to form $FeOD^+ + D$) have features that begin near 0.6 eV, even though both reactions are exothermic according to the known thermochemistry. Having discounted the possibility of an isomer, the simplest explanation for these observations is that there is a barrier associated with the four-centered transition state, as shown in Figure 5. Such a barrier would explain our inability to observe formation of $FeO^+ + D_2$ from the reaction of $Fe^+ + D_2O$. Because D_2 elimination from D–Fe^+–OD involves a tight four-centered transition state, this channel is kinetically less favorable than simple bond fission to form $FeOD^+ + D$. The addition of a potential energy barrier also makes formation of $FeO^+ + D_2$ much less favorable thermodynamically than $FeOD^+ + D$.

Another interesting observation regarding the $FeO^+ + D_2$ system is that the magnitude for endothermic formation of $FeOD^+ + D$ (reaction 7) is substantially larger than the magnitude for endothermic formation of $Fe^+ + D_2O$ (reaction 5a) even though the latter process is thermodynamically favored by over 1.0 eV. This is evidence for a tight transition state along the potential energy surface between the D–Fe^+–OD and Fe^+–OD_2 intermedi-

ates. Again, simple bond fission to form $FeOD^+$ is then kinetically favored compared with D_2O elimination. The height of this barrier may be indicated by the observation that the threshold for formation of $FeOD^+ + D$ from the $Fe^+(^4F) + D_2O$ reactants may be slightly above the thermodynamic threshold. Detailed phase space theory calculations for the analogous $CoO^+ + D_2$ reaction[20] indicate that this branching ratio is partially explained by statistical considerations, namely, that the density of rovibrational states for $CoOD^+$ increases more rapidly than that for D_2O. These calculations appear to indicate that the barrier between $Co^+ \cdot OD_2$ and D–Co^+–OD need not be large in order to explain the data. Similar considerations probably hold for the $FeO^+ + D_2$ system.

Although the potential energy surfaces shown in Figure 5 account nicely for most of the results, they fail to account for the small exothermic portion of the cross section corresponding to reaction 5a (Figure 2). We can think of four possible explanations for this behavior. First, there is an alternate pathway such as oxidative addition to the oxygen end of FeO^+. This possibility is rejected because there are good molecular orbital arguments against such a proposal,[17] and such pathways are also available to $CoO^+ + D_2$ where no exothermic reactivity is observed.[20] Second, the exothermic behavior is due to some contaminant, which need comprise only 0.14% of the ion beam to account for the magnitude of the exothermic portion of the cross section if it reacts on every collision. This contaminant could be a different chemical species at $m/z = 72$ amu (the nominal mass of FeO^+), potentially N_4O^+ reacting with D_2 to form N_4^+ (having the same mass as Fe^+) + D_2O. However, the same results were obtained when NO_2 was used as the oxidant in the flow tube, and we would expect that the magnitude of the exothermic reaction would differ depending on whether N_2O or NO_2 is present in the FT because this should influence the ratio of FeO^+ to N_4O^+. Third, a more likely "contaminant" is excited states of FeO^+ (either vibrational or electronic) that are not completely thermalized in the flow tube source before reaction, although we might have expected that the exothermic reactivity would vary when FeO^+ is made by reaction of Fe^+ with NO_2 or N_2O in the FT (processes that should populate internal FeO^+ states differently). This explanation is consistent with the enhanced exothermic reactivity observed by SFRS because the ion thermalization is less rigorous in the FTICR. The strongest argument against this possibility in the present experiments is that cooling of the FeO^+ with H_2 in the flow tube did not affect the reactivity with D_2 observed in the collision cell.[60] Fourth, there is another electronic surface that allows production of the D–Fe^+–OD intermediate without a reaction barrier. This possibility is consistent with the observation of similar behavior in the reaction of $FeO^+ + CH_4$[8] and is explored in more detail in the following section.

Electronic States of FeO^+ and the Activation Barrier. To understand why there is a barrier to the activation of D_2 by FeO^+, we consider the electronic character of the process by drawing analogy with the activation of a σ bond by a bare metal ion as discussed above and elsewhere.[17] The requirements are an empty orbital of suitable symmetry on the MO^+ molecule that can accept electron density from the σ bond of D_2, and an occupied orbital of π symmetry that can donate electron density into the σ^* bond of D_2. According to Fiedler et al.,[61] the FeO^+ molecule has a $^6\Sigma^+$ ground state and a $^4\Phi$ first excited state about 0.8 eV higher in energy. Our analysis indicates that these states have primary electron configurations of $8\sigma^2 3\pi^4 9\sigma^1 1\delta^2 4\pi^2$ and $8\sigma^2 3\pi^4 9\sigma^1 1\delta^3 4\pi^1$, respectively, where the 8σ and 3π orbitals are bonding, the 4π is antibonding, and the 9σ is largely 4s(Fe) in character. The lowest energy FeO^+ state having an empty 9σ is the $^4\Delta$, estimated to lie 1 eV above the $^6\Sigma^+$ state at a lower level of theory.[62]

In our previous analysis of the activation of D_2 by MO^+, we suggested that the 9σ orbital was the likely acceptor orbital, while either the 3π or 4π orbitals could act as the donor. If this hypothesis is correct, the surfaces shown qualitatively in Figure 6 result. the $^6\Sigma^+$ and $^4\Phi$ states of FeO^+ have barriers to D_2 activation because they both have occupied 9σ orbitals. Further, reaction of $FeO^+(^6\Sigma^+)$ with D_2 cannot form the quartet ground state of D–Fe^+–OD in a spin-allowed process. The lowest lying state of FeO^+ having the appropriate spin and electron configuration to efficiently activate the D_2 bond is the $^4\Delta$. The surface evolving from this state will cross those evolving from the $^4\Phi$, which should be more repulsive because the 9σ orbital is occupied. Even if the details of these ideas are incorrect, one of the low-lying quartet states of FeO^+ must evolve adiabatically to form the quartet state of D–Fe^+–OD. Reaction along the sextet surface can account for the bulk of the reactivity observed in Figure 2, because it passes over a 0.6-eV barrier and then proceeds to products along spin-allowed pathways. (As noted above, even if the sextet state of D–Fe^+–OD is below the quartet state in Figure 6, the experimental results are still explained as long as the barriers to elimination of D_2 and D_2O on either side of the intermediate are higher along the sextet surface than along the quartet surface.) Because we believe the sextet and quartet surfaces will cross one another, this provides a spin-forbidden path to form Fe^+. If this surface crossing is below the energy of the $FeO^+(^6\Sigma^+) + D_2$ asymptote, then ground-state reactants can form $Fe^+ + D_2O$ in a barrierless process that is inefficient because it is spin-forbidden. No exothermic formation of $FeOD^+ + D$ is observed within our experimental error, presumably because this reaction is much less exothermic than $Fe^+ + D_2O$ production. As noted above, it is also possible that the exothermic reactivity is due to the presence of small amounts of these low-lying quartet excited states. If this is true, the surface crossing need not be below the energy of the $FeO^+(^6\Sigma^+) + D_2$ asymptote. Clearly, theoretical calculations would remove some of the speculative nature of these surfaces.

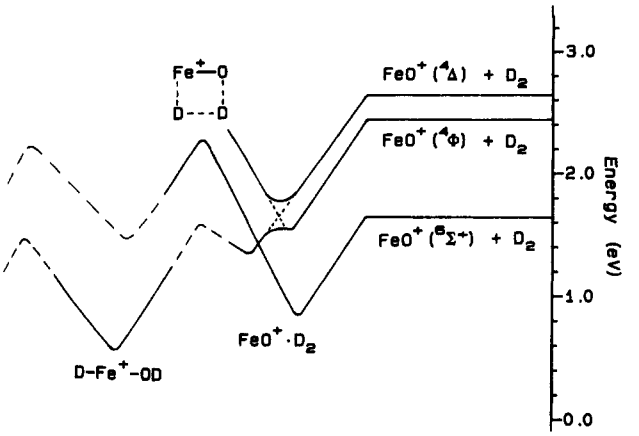

Figure 6. Semiquantitative potential energy diagram for the $[FeD_2O]^+$ system including speculative characterization of the electronic character of the $FeO^+ + D_2$ channel. Long dashed lines indicate a region of the potential energy surface where there is no quantitative experimental information. Short dashed lines indicate an avoided crossing between two diabatic quartet surfaces.

These surfaces are consistent with those derived for the reaction of CoO^+ with D_2 where the electronic details are believed to be very similar.[20] The only difference in the behavior of this system from that of $FeO^+ + D_2$ is that no exothermic reactivity is observed in the cobalt system. This could be because no electronically excited states of CoO^+ are present in the ion beam or because the spin-forbidden reaction is much less efficient. The latter situation could result if the crossing between the high-spin and low-spin surfaces or the barrier corresponding to the four-centered transition state on the low spin surface is above the $CoO^+ + D_2$ ground-state asymptote.

Summary

Cross sections for the reactions of $Fe^+(a^6D)$ and $Fe^+(a^4F)$ + D_2O and $FeO^+ + D_2$ are reported. In the Fe^+ system, reactions

to form $FeD^+ + OD$ and $FeOD^+ + D$ are observed in endothermic processes that result from a single collision. The a^4F state is found to be ~50 times more efficient than the a^6D state at producing FeD^+ and ~200 times more efficient at forming $FeOD^+$. Formation of FeO^+ is not observed for reaction of either state in the $Fe^+ + D_2O$ system. In the $FeO^+ + D_2$ reaction, formation of $Fe^+ + D_2O$ and $FeOD^+ + D$ occurs endothermically with thresholds of about 0.6 eV for both reaction channels even though existing thermochemistry indicates that these reactions are exothermic. Formation of FeD^+ at high energies is also observed in the $FeO^+ + D_2$ system but is a relatively minor process. A barrierless pathway to form $Fe^+ + D_2O$ is quite inefficient, occurring only once in every 600 collisions.

The most likely reaction mechanism for reaction of $Fe^+(a^4F) + D_2O$ and $FeO^+ + D_2$ involves formation of a D–Fe^+–OD insertion intermediate that has a quartet spin ground state. In the $FeO^+ + D_2$ reaction, molecular orbital ideas suggest that the D–Fe^+–OD intermediate is formed via a four-centered transition state. The similar thresholds observed for the $Fe^+ + D_2O$ and $FeOD^+ + D$ data channels are interpreted to mean that these reactions proceed over a common barrier associated with this transition state. The inefficiency of the reactivity of $Fe^+(a^6D) + D_2O$ is explained by noting that formation of this insertion intermediate is spin-forbidden. These reactants are then forced to transfer to the quartet surface, to react by a more inefficient direct atom abstraction mechanism, or to react along a higher energy sextet surface. We also speculate that the inefficient, barrierless channel for reaction 5a involves a spin-forbidden reaction.

Acknowledgment. This work is supported by the National Science Foundation, Grant CHE-9221241. We thank Detlef Schröder and Prof. Helmut Schwarz for communicating their results before publication.

References and Notes

(1) (a) Sheldon, R. A.; Kochi, J. K. *Metal-Catalyzed Oxidations of Organic Compounds*; Academic Press: New York, 1981.
(2) Sharpless, K. B.; Teranishi, A. Y.; Backvall, J. E. *J. Am. Chem. Soc.* **1977**, *99*, 3120.
(3) Sharpless, K. B.; Teranishi, A. Y. *J. Am. Chem. Soc.* **1971**, *93*, 2316.
(4) Wiberg, K. B. *Oxidation in Organic Chemistry*, Part A; Academic Press: New York, 1965.
(5) Jackson, T. C.; Jacobson, D. B.; Freiser, B. S. *J. Am. Chem. Soc.* **1984**, *106*, 1252.
(6) Schröder, D.; Schwarz, H. *Angew. Chem., Int. Ed. Engl.* **1990**, *29*, 1433.
(7) Schröder, D.; Fiedler, A.; Hrušák, J.; Schwarz, H. *J. Am. Chem. Soc.* **1992**, *114*, 1215.
(8) Chen, Y.-M.; Clemmer, D. E.; Armentrout, P. B. Manuscript in preparation.
(9) Elkind, J. E.; Armentrout, P. B. *J. Phys. Chem.* **1986**, *90*, 5736.
(10) Schultz, R. H.; Armentrout, P. B. *J. Phys. Chem.* **1987**, *91*, 4433.
(11) Hanton, S. D.; Noll, R. J.; Weisshaar, J. C. *J. Phys. Chem.* **1990**, *94*, 5655.
(12) Hanton, S. D.; Noll, R. J.; Weisshaar, J. C. *J. Chem. Phys.* **1992**, *96*, 5176.
(13) Armentrout, P. B. In *Gas Phase Inorganic Chemistry*; Russel, D. H., Ed.; Plenum: New York, 1989; p 1.
(14) Cassady, C. J.; Freiser, B. S. *J. Am. Chem. Soc.* **1984**, *106*, 6176.
(15) Murad, E. *J. Chem. Phys.* **1980**, *73*, 1381.
(16) Magnera, T. F.; David, D. E.; Michl, J. *J. Am. Chem. Soc.* **1989**, *111*, 4100.
(17) Clemmer, D. E.; Aristov, N.; Armentrout, P. B. *J. Phys. Chem.* **1993**, *97*, 544.
(18) Clemmer, D. E.; Sunderlin, L. S.; Armentrout, P. B. *J. Phys. Chem.* **1990**, *94*, 3008.
(19) Schröder, D.; Fiedler, A.; Ryan, M. F.; Schwarz, H. *J. Phys. Chem.* **1994**, *98*, 68.
(20) Chen, Y.-M.; Clemmer, D. C.; Armentrout, P. B. *J. Am. Chem. Soc.*, accepted for publication.
(21) Ervin, K. M.; Armentrout, P. B. *J. Chem. Phys.* **1985**, *83*, 166.
(22) Schultz, R. H.; Armentrout, P. B. *Int. J. Mass Spectrom. Ion Processes* **1991**, *107*, 29.
(23) Gerlich, D. In *State-Selected and State-to-State Ion-Molecule Reaction Dynamics. Part 1. Experiment*; Ng, C.-Y., Baer, M., Eds.; *Adv. Chem. Phys.* **1992**, *82*, 1.
(24) Chantry, P. J. *J. Chem. Phys.* **1971**, *55*, 2746.
(25) Sunderlin, L. S.; Armentrout, P. B. *J. Phys. Chem.* **1988**, *92*, 1209.
(26) van Koppen, P. A. M.; Kemper, P. R.; Bowers, M. T. *J. Am. Chem. Soc.* **1992**, *114*, 10941.
(27) Schultz, R. H.; Crellin, K. C.; Armentrout, P. B. *J. Am. Chem. Soc.* **1991**, *113*, 8590.
(28) Nitrogen oxide thermochemistry is taken from the JANAF tables: Chase, M. W., Jr.; Davies, C. A.; Downey, J. R., Jr.; Frurip, D. J.; McDonald, R. A.; Syverud, A. N. *J. Phys. Chem. Ref. Data* **1985**, *14* (Suppl. No. 1).
(29) Armentrout, P. B.; Halle, L. F.; Beauchamp, J. L. *J. Chem. Phys.* **1982**, *76*, 2449.
(30) Chen, Y.-M.; Armentrout, P. B. Unpublished results.
(31) Schultz, R. H.; Armentrout, P. B. *J. Chem. Phys.* **1992**, *96*, 10467.
(32) Khan, F. A.; Clemmer, D. C.; Schultz, R. H.; Armentrout, P. B. *J. Phys. Chem.* **1993**, *97*, 7978.
(33) Fisher, E. R.; Kickel, B. L.; Armentrout, P. B. *J. Phys. Chem.* **1993**, *97*, 10204.
(34) Fisher, E. R.; Kickel, B. L.; Armentrout, P. B. *J. Chem. Phys.* **1992**, *97*, 4859.
(35) Dalleska, N. F.; Honma, K.; Armentrout, P. B. *J. Am. Chem. Soc.* **1993**, *115*, 12125.
(36) Chen, Y.-M.; Armentrout, P. B. *Chem. Phys. Lett.* **1993**, *210*, 123.
(37) Chen, Y.-M.; Clemmer, D. E.; Armentrout, P. B. *J. Chem. Phys.* **1991**, *95*, 1228.
(38) Armentrout, P. B. In *Advances in Gas Phase Ion Chemistry*; Adams, N. G., Babcock, L. M., Eds.; JAI: Greenwich, 1992; Vol. 1, p 83.
(39) Weber, M. E.; Elkind, J. L.; Armentrout, P. B. *J. Chem. Phys.* **1986**, *84*, 1521.
(40) Clemmer, D. E.; Sunderlin, L. S.; Armentrout, P. B. *J. Phys. Chem.* **1990**, *94*, 208.
(41) The a^6D state comprises ~78% of the SI beam and ~97% of the FT beam. This change in population between the two sources is a factor of ~1.2 and is near the ±20% limit in the uncertainty of the cross section magnitudes in these experiments.
(42) Fisher, E. R.; Elkind, J. L.; Clemmer, D. E.; Georgiadis, R.; Loh, S. K.; Aristov, N.; Sunderlin, L. S.; Armentrout, P. B. *J. Chem. Phys.* **1990**, *93*, 2676.
(43) Armentrout, P. B.; Kickel, B. L. In *Organometallic Ion Chemistry*; Freiser, B. S., Ed.; VCH: New York, in press.
(44) Elkind, J. L.; Armentrout, P. B. *J. Phys. Chem.* **1987**, *91*, 2037.
(45) Gioumousis, G.; Stevenson, D. P. *J. Chem. Phys.* **1958**, *29*, 292.
(46) Kappes, M. M.; Staley, R. H. *J. Phys. Chem.* **1981**, *85*, 942.
(47) Armentrout, P. B.; Halle, L. F.; Beauchamp, J. L. *J. Am. Chem. Soc.* **1981**, *103*, 6501.
(48) Mandich, M. L.; Halle, L. F.; Beauchamp, J. L. *J. Am. Chem. Soc.* **1984**, *106*, 4403.
(49) Elkind, J. L.; Armentrout, P. B. *Inorg. Chem.* **1986**, *25*, 1078.
(50) For recent reviews, see: Armentrout, P. B. *Science* **1991**, *251*, 175; *Annu. Rev. Phys. Chem.* **1990**, *41*, 313; In *Selective Hydrocarbon Activation: Principles and Progress*; Davies, J. A., Watson, P. L., Greenberg, A., Liebman, J. F., Eds.; VCH: New York, 1990; p 467.
(51) Rosi, M.; Bauschlicher, C. W.; Langhoff, S. R.; Partridge, H. *J. Phys. Chem.* **1990**, *94*, 8656.
(52) Fiedler, A.; Schröder, D.; Shaik, S.; Schwarz, H. *J. Am. Chem. Soc.*, submitted for publication.
(53) $FeOD^+$ should have a quintet ground state if one assumes that the Fe^+ forms one covalent bond with the OD ligand and that the other metal electrons remain spin decoupled, as in FeD^+ and the isoelectronic $FeCH_3^+$. Both species have been calculated to have quintet ground states. See: Bauschlicher, C. W.; Langhoff, S. R. *Int. Rev. Phys. Chem.* **1990**, *9*, 149.
(54) Aristov, N.; Armentrout, P. B. *J. Phys. Chem.* **1987**, *91*, 6178.
(55) Schultz, R. H.; Armentrout, P. B. *J. Phys. Chem.* **1993**, *97*, 596.
(56) Marinelli, P. J.; Squires, R. R. *J. Am. Chem. Soc.* **1989**, *111*, 4101.
(57) Rosi, M.; Bauschlicher, C. W. *J. Chem. Phys.* **1989**, *90*, 7264; **1990**, *92*, 1876.
(58) The calculations do not reproduce the experimental splitting between the ^6D and ^4F states of atomic Fe^+. If the calculations are corrected for this difference, the $^4A_1$ state of $FeOH_2^+$ will lie only 0.03 eV above the $^6A_1$ state.
(59) Irikura, K. K.; Beauchamp, J. L. *J. Am. Chem. Soc.* **1989**, *111*, 75.
(60) Experiments in which the FeO^+ was attenuated by H_2 to as much as 50% did not affect the exothermic reactivity observed.
(61) Fiedler, A.; Hrušák, J.; Koch, W.; Schwarz, H. *Chem. Phys. Lett.* **1993**, *211*, 242.
(62) Krauss, M.; Stevens, W. J. *J. Chem. Phys.* **1985**, *82*, 5584.